Annals of Pharmacy Practice and Pharmacotherapy
ISSN: 3062-4436
2025, Volume 5, Page No: 201-221

Available online at: www.galaxypub.co/page/journals

Galaxy Publication

Glucocorticoid Receptor-Dependent Suppression of Hippocampal Cytochrome P450 by Pregnenolone 16α-Carbonitrile Attenuates Phenytoin-Induced Neurotoxicity

Thabo M. Nkosi[1], Lerato P. Maseko[1]*

[1]Department of Pharmacy Practice, School of Pharmacy, University of Pretoria, Pretoria, South Africa.

***E-mail** ✉ l.maseko_pharm@gmail.com

Received: 12 January 2025; **Revised:** 27 March 2025; **Accepted:** 03 April 2025

ABSTRACT

The cytochrome P450 (CYP) enzyme system plays an important role in regulating neurophysiological processes within the central nervous system through its involvement in neurosteroid metabolism. Phenytoin (PHT), a commonly used antiepileptic drug, has been associated with adverse neuronal effects, which may result from its ability to induce CYP expression and alter testosterone (TES) metabolism in the hippocampus. Although the pregnane X receptor (PXR) is well recognized for its role in controlling hepatic CYP expression, our findings reveal that pregnenolone 16α-carbonitrile (PCN), a PXR agonist, exerts distinct regulatory effects on CYP expression in the liver compared with the hippocampus in mice. PCN administration increased the expression of CYP3A11 and CYP2B10 in the liver but led to a reduction of these enzymes in the hippocampus. Importantly, PCN treatment alleviated PHT-induced hippocampal neuronal damage, which was associated with suppressed TES metabolism in the hippocampus. Further mechanistic investigations demonstrated that the downregulation of hippocampal CYP expression and the protective effects of PCN against PHT-induced neurotoxicity were mediated by the glucocorticoid receptor rather than PXR, as confirmed through both genetic and pharmacological approaches. Overall, this study demonstrates that PCN can suppress CYP expression in the hippocampus and reduce PHT-induced neurotoxicity through a PXR-independent mechanism. These results indicate that glucocorticoids may offer a promising therapeutic approach for mitigating the neurological side effects associated with PHT treatment.

Keywords: Pregnane X receptor, Pregnenolone 16α-carbonitrile, Glucocorticoid receptor, Hippocampus, Phenytoin sodium, Neurotoxicity

How to Cite This Article: Nkosi TM, Maseko LP. Glucocorticoid Receptor-Dependent Suppression of Hippocampal Cytochrome P450 by Pregnenolone 16α-Carbonitrile Attenuates Phenytoin-Induced Neurotoxicity. Ann Pharm Pract Pharmacother. 2025;5:201-21. https://doi.org/10.51847/dbkV1db2TX

Introduction

Cytochrome P450 enzymes (CYPs) comprise a group of heme-based monooxygenases that facilitate oxidative biochemical reactions and are essential for the metabolism of endogenous molecules as well as foreign compounds [1]. While CYP activity is most prominent in peripheral organs such as the liver and intestine, a wide range of CYP isoforms is also expressed in the central nervous system. Within the brain, these enzymes contribute to the biotransformation of neurosteroids and numerous xenobiotics, including psychoactive medications [2].

The hippocampus is a central structure involved in cognitive processing, emotional regulation, and memory consolidation. Several CYP isoforms, including CYP3A, CYP2B, and CYP2C, are present in hippocampal tissue [3, 4]. Disruption of CYP homeostasis in the brain has been implicated in drug-related neurotoxicity. Notably, treatment with the antiepileptic agent phenytoin (PHT) elevates CYP expression in the hippocampus, thereby accelerating CYP-dependent testosterone (TES) metabolism. This enhanced metabolism impairs hippocampal neurogenesis and compromises neuronal survival [5-10]. These molecular changes may explain the depressive symptoms and cognitive dysfunction observed clinically in patients receiving PHT. Consistent with this notion, both experimental and clinical investigations have established the neuroprotective role of TES [11, 12].

The transcriptional induction of CYP enzymes by drugs or xenobiotics is primarily governed by ligand-activated nuclear receptors, including constitutive androstane receptor (CAR), pregnane X receptor (PXR), and glucocorticoid receptor (GR). These receptors are well characterized for their regulatory functions in hepatic and intestinal CYP expression. For example, PHT has been shown to induce human CYP2B6 [13] and murine CYP2C29 [14] through CAR-mediated pathways. Mechanistically, PHT promotes CAR activation and nuclear translocation, enabling CAR to interact with phenobarbital-responsive enhancer elements within the CYP2B6 gene and stimulate transcription [13]. Although these nuclear receptors are also expressed in the brain [15], their contribution to the regulation of CYP expression in the central nervous system remains poorly defined. In particular, whether PXR signaling in the brain influences CYP-mediated TES metabolism and contributes to the neurological adverse effects associated with PHT has not been adequately investigated.

In the present study, we demonstrate that pregnenolone 16α-carbonitrile (PCN), a classical PXR agonist, reduces PHT-induced neurotoxicity in the hippocampus by selectively downregulating hippocampal CYP expression. Importantly, this protective effect occurs independently of PXR activation and instead appears to involve glucocorticoid (GC)–glucocorticoid receptor (GR) signaling.

Materials and Methods

Animals and drug administration

Male C57BL/6J mice (6–8 weeks old; 20 ± 2 g) were obtained from the Animal Center of Hubei Province, China (Permit No.: SCXK 2015-0018) and maintained under specific pathogen-free conditions. All experimental procedures were approved and carried out at the Animal Experimental Center of Wuhan University (Permit No.: 14016), an institution accredited by the Association for Assessment and Accreditation of Laboratory Animal Care International. Animal handling and experimental protocols conformed to the standards established by the Chinese Council on Animal Welfare for Laboratory Animal Use. Mice were housed in a controlled environment with a temperature of 18–22 °C, humidity of 40–60%, adequate ventilation, and a 12 h light/dark cycle. In parallel, male PXR knockout (KO) mice of the same age and weight range, generated on a C57BL/6J background as previously described [16], were included in the study.

Following a one-week acclimation period, animals received intraperitoneal injections of the designated compounds. The treatment groups were as follows: (1) PHT (Sigma-Aldrich, St. Louis, MO, USA) administered at 20 mg/kg daily for 28 days, a dosage selected based on previously established ranges associated with antiepileptic efficacy and neurotoxicity in rodents, as well as the requirement for prolonged exposure [17-19]; (2) PCN (Houston, APExBIO, TX, USA) given at 15 mg/kg every three days for a total of nine administrations over 28 days, based on prior evidence indicating the need for higher doses to achieve central nervous system penetration [20, 21]; (3) dexamethasone (DEX; Sigma-Aldrich) administered at 4 mg/kg concurrently with PCN every three days for nine total doses, informed by earlier studies demonstrating anticonvulsant effects at lower doses and neurotoxicity at higher doses [22, 23]; and (4) mifepristone (RU486; APExBIO) administered at 10 mg/kg, a dose shown to exert anti-glucocorticoid effects and cross the blood–brain barrier [24].

Behavioral assessment

Only male mice were used to avoid variability associated with the estrous cycle. Animals were allowed to habituate to the behavioral testing environment for one week prior to testing. All behavioral experiments were conducted between 8:00 a.m. and 6:00 p.m.

Elevated plus maze

The elevated plus maze consisted of two open arms and two enclosed arms extending from a central platform. To eliminate olfactory cues, the apparatus was thoroughly cleaned with 75% ethanol before each trial. Mice were placed on the central platform and permitted to explore the maze freely for 5 min. Behavioral parameters were recorded and analyzed using the SMART 3.0 tracking system (Holliston, Panlab, MA, USA).

Open field test

The open field apparatus was a black, square arena in which each mouse was positioned at the center at the beginning of the test. Locomotor activity was recorded for 5 min using a video tracking system. The arena was

virtually divided into 25 equal squares, allowing quantitative assessment of movement patterns and depression-related behaviors based on grid exploration.

Morris water maze

The apparatus was a circular pool with opaque black walls, virtually segmented into four equivalent quadrants. An escape platform was positioned in a fixed quadrant, submerged 2–4 cm beneath the water surface to remain invisible. The protocol included an acquisition phase followed by a probe trial. During acquisition, mice were released into the pool from each of the four quadrant starting points in turn, always facing the wall, in water maintained at 22 ± 1 °C. An overhead camera captured swimming trajectories for up to 90 s per trial. Mice that did not reach the platform within 60 s were gently placed onto it. Training consisted of four trials per day over four consecutive days. On the fifth day, a single trial from a designated quadrant measured escape latency. In the probe trial, the platform was removed entirely, and swimming patterns were recorded for 60 s to evaluate memory retention.

Real-time quantitative reverse transcription-polymerase chain reaction (RT-qPCR)

RNA was extracted from samples with QIAzol Lysis Reagent (Qiagen, Hilden, Germany), followed by removal of contaminating genomic DNA using TURBO-DNase (Ambion, Austin, TX, USA). Complementary DNA was synthesized with the iScript™ cDNA Synthesis Kit (Bio-Rad, Hercules, CA, USA). Quantification of transcript levels employed the ΔΔCq approach on an Applied Biosystems 7300 platform (Applied Biosystems, Bedford, MA, USA) using iTaq SYBR Green Supermix with ROX (Bio-Rad). Expression data were normalized to the reference gene glyceraldehyde 3-phosphate dehydrogenase (Gapdh).

Western blotting

Hippocampi were isolated immediately after sacrifice on an ice-cold surface, flash-frozen in liquid nitrogen, and kept at −80 °C pending analysis. Samples were later thawed on ice and lysed in five volumes of chilled buffer (PBS; PWL101, Meilunbio, Dalian, China) containing 0.2% NP-40 plus protease inhibitors. After centrifugation (15, 000 g, 20 min, 4 °C), supernatant protein content was determined by bicinchoninic acid assay. Proteins (25 μg per lane) were denatured in loading buffer (Bio-Rad), resolved on 15% SDS-polyacrylamide gels, and electroblotted onto polyvinylidene fluoride membranes. Membranes were probed overnight with primary antibodies directed against CYP3A11 (1:500, gift from Dr. Frank J. Gonzalez, NIH, USA), CYP2B10 (1:1, 500, Sigma-Aldrich), β-actin (1:1, 000, Santa Cruz Biotechnology, Santa Cruz, CA, USA), or GAPDH (1:2, 000, Abclonal, Wuhan, China), then with horseradish peroxidase-linked secondary antibodies (1:20, 000, BD Diagnostic Systems, Sparks, MD, USA). Signals were developed using enhanced chemiluminescence reagent (Thermo Fisher Scientific Inc., Waltham, MA, USA) and quantified densitometrically with ImageJ (NIH-Image 1.42q, Bethesda, MD, USA). Target band intensities were expressed relative to β-actin or GAPDH.

Nissl staining

Brain specimens were immersed in 4% paraformaldehyde at 4 °C for 18 h, cryoprotected in optimum cutting temperature compound, and stored at −80 °C. Coronal sections (35 μm) were prepared on a sliding microtome (CM1950, Leica Microsystems GmbH, Wetzlar, Germany). After rinsing in pH 7.4 PBS, sections were dried at 55 °C for 3 h, then stained with 0.9% crystal violet (Sigma-Aldrich) at 37 °C for 2 h. Gradual dehydration was achieved through ascending ethanol concentrations (70–100%, 5 min each), and sections were coverslipped with neutral balsam. Imaging was performed on a fluorescence microscope (Eclipse 80i, Nikon Corporation, Tokyo, Japan; scale bar 100 μm). Nissl substance-positive cell area and optical density were measured using ImageJ.

Golgi staining

Hippocampal neuronal architecture was examined via rapid Golgi impregnation using a commercial kit (FD NeuroTechnologies, Ellicott City, MD, USA) per the supplied protocol. Dendritic spines were counted within the initial 15–30 μm segment of primary apical dendrites. Analysis was restricted to fully impregnated neurons displaying unambiguous somatic contours and higher-order branching; selection was random within defined hippocampal fields. Spine numbers were normalized to density per 10 μm of dendrite. Dendritic complexity was assessed by Sholl analysis of intersection counts and primary branch order. Images of five neurons per section (three sections per animal) were acquired with Nikon act-1 software and evaluated blindly in ImageJ. Cumulative

Sholl intersections were tallied out to 150 μm from the cell body, and primary branch counts were recorded separately.

Immunohistochemistry (IHC)

Protein localization in brain tissue was investigated by immunohistochemistry. Whole brains were fixed overnight in Hartman's solution (Sigma-Aldrich), cryoprotected at −80 °C in optimum cutting temperature compound, and sectioned at 15 μm thickness. Sections were blocked with 10% bovine serum albumin overnight at 4 °C before overnight incubation with primary antibodies recognizing CYP3A11 (1:200, gift from Dr. Frank J. Gonzalez, NIH, USA), CYP2B10 (1:300, Sigma-Aldrich), PXR (1:100, ab217375, Abcam, Cambridge, MA, USA), or GR (1:150, ab3578, Abcam). Biotinylated secondary antibody (1:3, 000, BA9500, Vector Laboratories, Newark, CA, USA) was applied for 3 h at room temperature, followed by avidin-biotin complex reagent (1:200, PK-6100, Vector Laboratories) for 3 min in darkness. Slides were coverslipped with neutral balsam. Quantitative assessment utilized the IHC-Toolbox plugin in ImageJ [25], employing color deconvolution to isolate positive staining and derive gray-scale intensity values. Positive cell fractions were calculated with IHC-Toolbox and IHC Profiler; cells exhibiting >65% stained area were scored positive.

Liquid chromatography-tandem mass spectrometry (LC-MS/MS)

Levels of testosterone (TES) and its metabolite 6β-hydroxytestosterone (6β-OH-TES) were measured in brain homogenates and serum by LC-MS/MS. Tissue extraction employed diethyl ether as reported previously [26]. Separations were conducted on a two-dimensional LC system interfaced with an AB/Sciex QTrap 5500 mass spectrometer (SCIEX, Framingham, MA, USA) using atmospheric pressure chemical ionization (positive mode) and electrospray ionization (negative mode). Analytes were detected directly without derivatization. For kinetic studies of testosterone hydroxylation, microsomal fractions were isolated by ultracentrifugation to retain CYP activity [27]. Reactions (200 μL total volume) contained Tris-HCl buffer (50 mM Tris, 150 mM KCl, 10 mM $MgCl_2$, pH 7.4), 1.25 mM NADPH, 0.5 mg/mL microsomal protein, and substrate at concentrations ranging from 25 to 375 μM. Metabolism was started by NADPH addition at 37 °C and quenched with ice-cold acetonitrile.

Bioinformatic analysis of gene expression omnibus (GEO) microarray data

Microarray data from GEO accession GSE2880 were re-analyzed. Hippocampal expression profiles from phenytoin (PHT)-exposed animals and vehicle controls were compared. Differentially expressed genes were identified with the limma R package. Glucocorticoid receptor (GR) target genes curated from published literature were highlighted in volcano plots generated by EnhancedVolcano. Genes meeting criteria of $|logFC| > 0.5$ and $P < 0.05$ underwent pathway enrichment using ClusterProfiler. Complete analysis scripts are hosted on GitHub.

Statistical analysis

Data were analyzed in GraphPad Prism version 9.1.1 (GraphPad Software, San Diego, CA, USA). Pairwise comparisons used two-tailed Student's t-tests; multi-group datasets were evaluated by one-way ANOVA with Bonferroni post-hoc correction. Datasets with two factors were examined by two-way ANOVA. Longitudinal measures employed repeated-measures ANOVA. Significance was set at $P < 0.05$. Results are reported as mean ± standard error of the mean.

Results and Discussion

PCN reduces CYP levels in the hippocampus regardless of PXR activity

To determine whether PXR signaling within the brain contributes to the regulation of cytochrome P450 enzymes, mice were exposed to pregnenolone 16α-carbonitrile (PCN), a canonical activator of mouse PXR, followed by assessment of CYP expression in distinct tissues. In line with its established hepatic action, PCN administration led to a robust elevation of CYP3A11 and CYP2B10 transcripts in the liver **(Figure 1a)**. However, examination of hippocampal tissue from the same animals revealed the opposite response: expression of both CYP genes was markedly reduced.

This divergent response highlights a clear tissue-dependent effect of PCN, in which peripheral and central tissues respond in opposing directions. To confirm that this phenomenon extended beyond transcriptional changes, protein localization and abundance were examined by immunohistochemistry. Enhanced CYP3A11 and

CYP2B10 immunoreactivity was detected in liver sections following PCN treatment (**Figure 1b**). In contrast, hippocampal regions associated with learning and memory, including the cornu ammonis 1 (CA1) and dentate gyrus (DG), displayed a pronounced loss of CYP3A11 and CYP2B10 staining (**Figure 1c**).

Collectively, these findings demonstrate that PCN acts as a suppressor of CYP expression within the hippocampus, despite its inductive role in the liver. This opposing regulation suggests that the hippocampal effects of PCN are not mediated through canonical PXR signaling pathways.

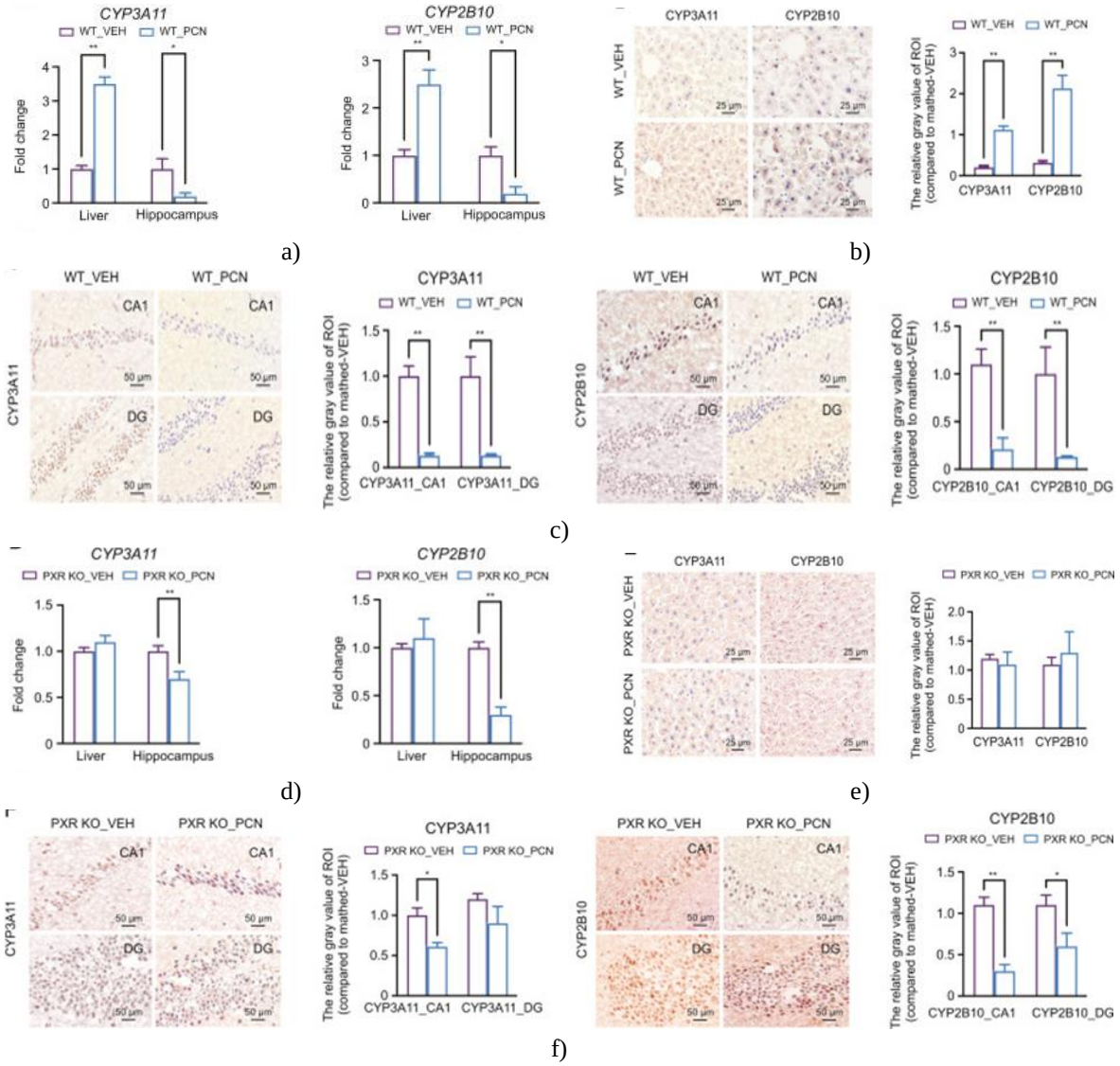

Figure 1. Pregnenolone 16α-carbonitrile (PCN) reduces cytochrome P450 enzyme levels in the hippocampus through a mechanism that does not require pregnane X receptor (PXR). (a−c) Adult male wild-type (WT) mice (n = 6) received daily doses of either vehicle (VEH) or PCN over four weeks before organs were collected. Levels of mRNA for cytochrome P450 isoforms CYP3A11 and CYP2B10 were quantified by RT-qPCR in liver and hippocampal tissues (a). Protein distribution was assessed via immunohistochemical staining for CYP3A11 and CYP2B10 in liver sections (b) and hippocampal sections (c). (d−f) In PXR-null (PXR KO) mice (n = 6) treated identically with VEH or PCN for four weeks, RT-qPCR measured CYP3A11 and CYP2B10 transcripts in liver and hippocampus (d), while IHC visualized the corresponding proteins in liver (e) and hippocampus (f). Semi-quantitative analysis of IHC images was performed using ImageJ with IHC-Toolbox plugins. Values are expressed as mean ± SEM. ∗P < 0.05; ∗∗P < 0.01. ROI: region of interest; CA1: cornu ammonis 1; DG: dentate gyrus.

To investigate the role of PXR in PCN-driven downregulation of brain cytochrome P450 enzymes, experiments were extended to PXR knockout animals. Consistent with PXR's established function, PCN no longer stimulated

hepatic transcription of CYP3A11 or CYP2B10 in the absence of this receptor **(Figure 1d)**. Remarkably, however, PCN still markedly lowered mRNA abundance of both enzymes within the hippocampus of knockout mice, revealing a clear PXR-independent pathway for this brain-specific repression. Protein-level confirmation came from IHC examination of CYP3A11 and CYP2B10 in liver (**Figure 1e**) and hippocampal regions (**Figure 1f**) of knockout animals, where the inhibitory profile closely resembled that seen in wild-type counterparts. Taken together, these data establish that PCN curbs hippocampal cytochrome P450 activity via routes unrelated to PXR activation.

PCN blocks phenytoin-elicited upregulation of hippocampal cytochrome P450 enzymes without relying on PXR

Clinical use of the anticonvulsant phenytoin (PHT) has been associated with mood disorders and memory problems in subsets of patients [6, 28], complications linked to heightened hippocampal CYP3A activity and accelerated breakdown of testosterone (TES) [29, 30]. Prolonged PHT exposure notably elevates CYP3A11 in CA1 neurons while promoting CYP3A-catalyzed TES clearance [29]. We therefore tested whether concurrent PCN delivery could counteract PHT-triggered cytochrome P450 induction in the hippocampus. Wild-type mice were assigned to vehicle, PHT monotherapy, or combined PHT/PCN regimens. Hepatic transcription of CYP3A11 and CYP2B10 rose substantially with PHT alone, as anticipated **(Figure 2a)**. Adding PCN exerted negligible influence on CYP3A11 transcript levels in liver but amplified the rise in CYP2B10 mRNA **(Figure 2a)**. Within the hippocampus, PHT monotherapy reliably boosted transcription of both CYP isoforms, aligning with published evidence [29]. Critically, PCN co-delivery substantially dampened this PHT-induced hippocampal elevation for CYP3A11 and CYP2B10 **(Figure 2a)**. Parallel changes at the protein level in liver (**Figures 2b, 2d** left panels) and hippocampus (**Figures 2b, 2d** right panels) were substantiated through IHC and Western blot analyses. Overall, these results highlight PCN's potential to offset PHT-related hippocampal disturbances by interfering with the anticonvulsant's ability to ramp up local cytochrome P450 expression.

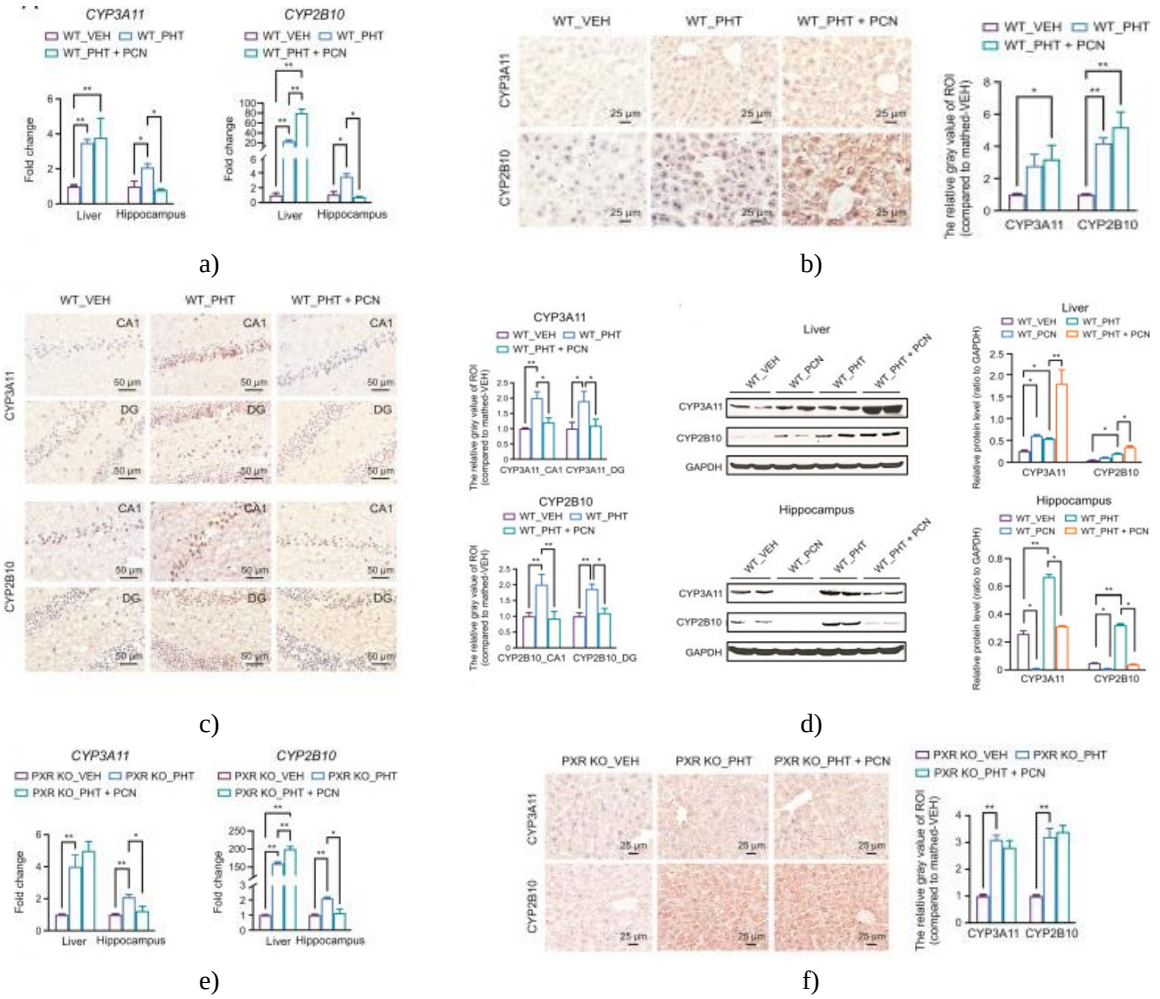

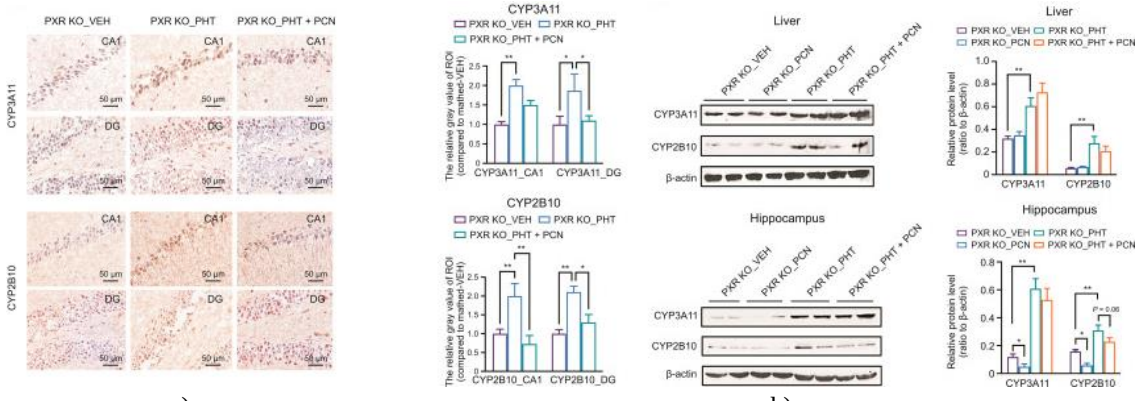

Figure 2. Pregnenolone 16α-carbonitrile (PCN) counteracts the phenytoin (PHT)-induced upregulation of cytochrome P450 enzymes in the hippocampus through a pregnane X receptor (PXR)-independent pathway. (A–D) Adult male wild-type (WT) mice (n = 6) received daily administration of vehicle (VEH), PHT alone, PCN alone, or combined PHT + PCN for four weeks prior to tissue collection. Messenger RNA (mRNA) levels of cytochrome P450 isoforms CYP3A11 and CYP2B10 were determined by RT-qPCR in liver and hippocampal samples (a). Protein localization was evaluated by immunohistochemical (IHC) staining for CYP3A11 and CYP2B10 in liver (b) and hippocampal sections (c). Western blot analysis quantified CYP3A11 and CYP2B10 protein abundance in both tissues (d). (e–h) Identical treatments were applied to PXR knockout (PXR KO) mice (n = 6). RT-qPCR assessed CYP3A11 and CYP2B10 transcripts in liver and hippocampus (e), while IHC visualized the proteins in liver (f) and hippocampus (g), and Western blotting confirmed protein levels across tissues (h). IHC images were semi-quantitatively analyzed using ImageJ with IHC-Toolbox plugins. Results are displayed as mean ± SEM. ∗P < 0.05; ∗∗P < 0.01. ROI: region of interest; CA1: cornu ammonis area 1; DG: dentate gyrus; GAPDH: glyceraldehyde 3-phosphate dehydrogenase.

To assess whether PCN's ability to blunt PHT-driven hippocampal CYP upregulation relies on PXR, the same treatment protocols were applied to PXR knockout mice. In these animals, PHT still elevated hepatic mRNA levels of CYP3A11 and CYP2B10 **(Figure 2e)**. Co-administration of PCN did not alter the magnitude of CYP3A11 induction compared to PHT alone, though it caused a modest but significant additional rise in CYP2B10 transcripts **(Figure 2e)**. The basis for this extra CYP2B10 boost in the PHT + PCN group is unclear, but prolonged PCN exposure in the absence of PXR might indirectly promote constitutive androstane receptor (CAR) activity. Within the hippocampus, PHT robustly increased transcription of both CYP3A11 and CYP2B10, yet these elevations were substantially reduced by concurrent PCN delivery **(Figure 2e)**. Matching patterns were observed at the protein level in liver (**Figures 2f, 2h** left panels) and hippocampal tissues (**Figures 2g, 2h** right panels), as validated by IHC and Western blotting. Overall, these data demonstrate that PCN opposes PHT-induced hippocampal CYP elevation via PXR-independent mechanisms.

PCN administration mitigates the neurological adverse effects associated with PHT

Since PHT's neurotoxic side effects are largely linked to excessive hippocampal CYP activity and accelerated testosterone (TES) catabolism, we explored whether PCN could alleviate these issues by lowering CYP levels and preserving TES bioavailability. In particular, we tested if PCN co-treatment could counteract PHT's detrimental impact on hippocampal TES homeostasis and associated behavioral/histological deficits.

A PHT-induced neurotoxicity model was generated by administering the drug to 6-week-old male mice for four weeks, followed by comprehensive neurobehavioral assessments. The Morris water maze revealed marked cognitive deficits in PHT-treated animals, including prolonged escape latencies during training and reduced time spent in the target quadrant along with fewer platform crossings during the probe trial. In the elevated plus maze, PHT exposure significantly shortened open-arm dwell time compared to vehicle controls, reflecting heightened anxiety-like behavior. Open-field testing further indicated diminished exploratory drive, with less central zone occupancy but greater peripheral activity. Collectively, these outcomes confirm that chronic PHT provokes deficits in learning/memory, anxiety-related responses, and locomotion patterns.

Histopathological examination via Nissl staining of hippocampal sections showed fewer Nissl-positive neurons in the CA1 and CA3 subfields of PHT-treated mice relative to controls. A similar downward trend, though non-

significant, was noted in the dentate gyrus (DG). Whole-hippocampus densitometry confirmed reduced staining intensity overall. Notably, CA3 neurons from PHT animals displayed central chromatolysis—characterized by loss of centrally located Nissl substance and peripheral clumping—along with cytoplasmic vacuolization, pointing to impaired protein synthesis. Supporting this, hippocampal mRNA levels of synaptic markers PSD95, SYN1, SYP, and SYT1 were downregulated in the PHT group. These observations indicate that PHT neurotoxicity involves structural damage, neuronal loss, and disrupted synaptic protein expression in the hippocampus.

CYP3A enzymes are primary catalysts converting TES into the weakly active metabolite 6β-hydroxytestosterone (6β-OH-TES), thereby inactivating the hormone [31]. To isolate brain-specific effects and bypass hepatic contributions, TES and 6β-OH-TES concentrations were quantified directly in hippocampal tissue. Preliminary in vitro assays confirmed robust testosterone-metabolizing capacity in microsomes from both liver and hippocampus. Kinetic studies on hippocampal microsomes revealed that PHT enhanced TES turnover, whereas PCN mildly slowed it. In liver microsomes, both compounds accelerated metabolism. In vivo, PHT elevated the hippocampal 6β-OH-TES/TES ratio, reflecting heightened local CYP activity, an effect that PCN fully reversed **(Figure 3a)**. Thus, PHT promotes intrahippocampal TES degradation, and PCN co-administration effectively restores TES balance by curbing this process.

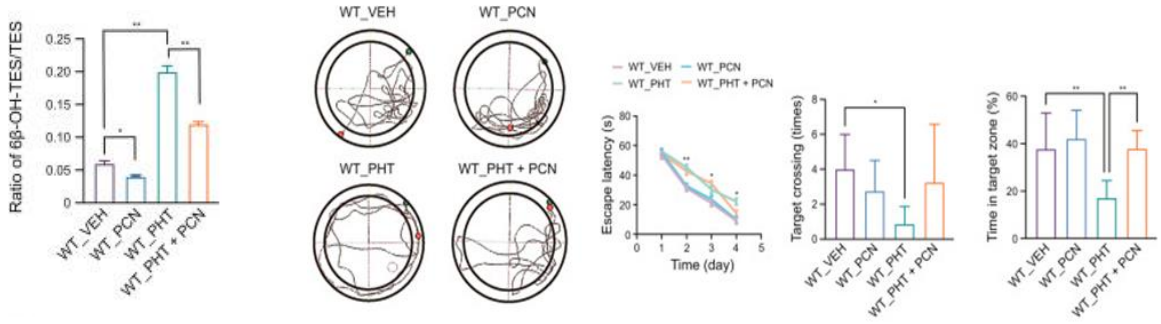

a) b)

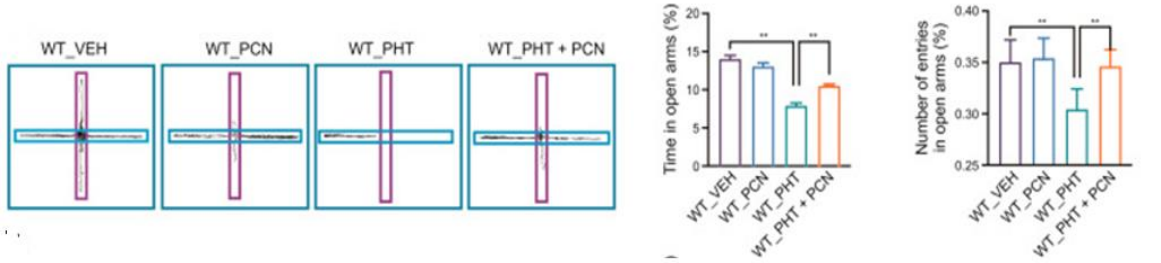

c)

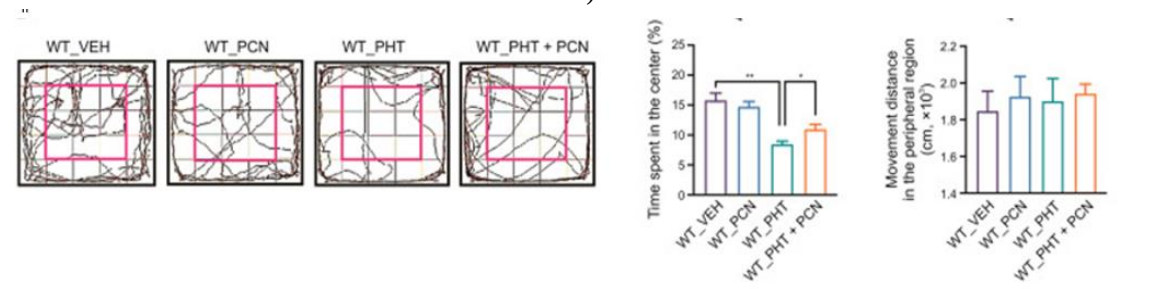

d)

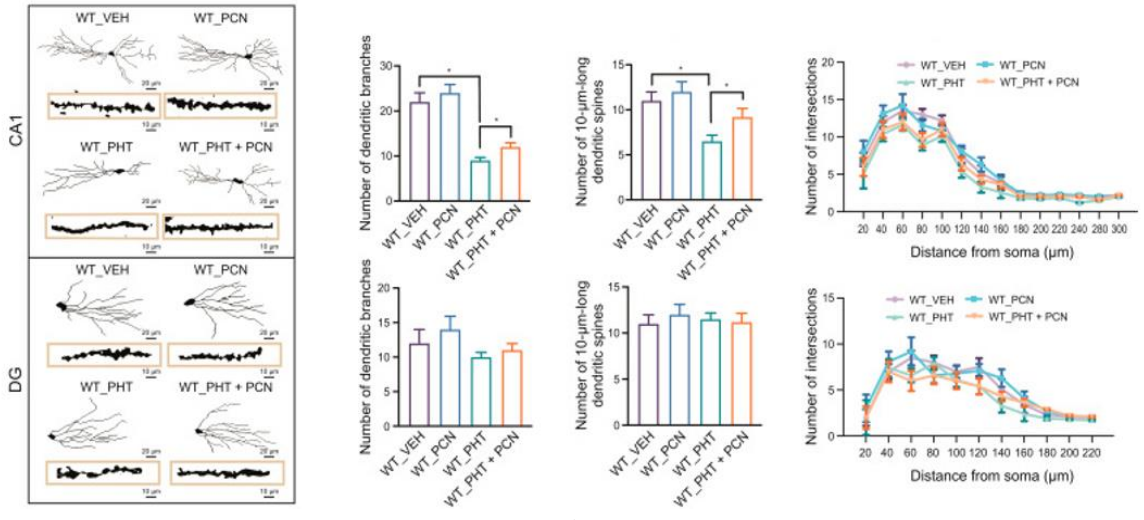

e)

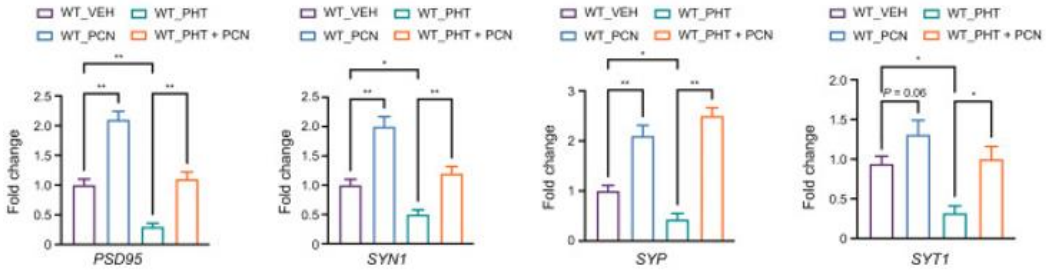

f)

Figure 3. Pregnenolone 16α-carbonitrile (PCN) mitigates the neurotoxic consequences of phenytoin (PHT) exposure. Adult male wild-type (WT) mice (n = 8) received daily treatment with vehicle (VEH), PCN alone, PHT alone, or combined PHT + PCN for four weeks prior to testing. (a) Hippocampal ratio of 6β-hydroxytestosterone (6β-OH-TES) to testosterone (TES), quantified by liquid chromatography-tandem mass spectrometry. (b) Morris water maze performance, showing escape latency during training, along with platform crossings and time spent in the target quadrant during the probe trial. (c) Elevated plus maze outcomes, including representative movement tracks, duration, and entries into open arms. (d) Open-field test metrics, comprising time spent in the central zone and distance traveled in the peripheral zone. (e) Golgi-impregnated hippocampal sections with representative neurite tracings from cornu ammonis area 1 (CA1) and dentate gyrus (DG) neurons; quantitative analyses focused on branch number, dendritic spine density, and branch nodes. (f) Hippocampal mRNA levels of synaptic markers PSD95, SYN1, SYP, and SYT1, determined by RT-qPCR. Results are expressed as mean ± SEM. ∗P < 0.05; ∗∗P < 0.01.

Reduced neurosteroid availability, particularly of TES, has been linked to the neurological adverse effects of PHT [29]. The present data support the idea that PHT-driven upregulation of hippocampal cytochrome P450 enzymes promotes excessive TES inactivation, thereby contributing to the observed behavioral deficits and hippocampal damage. In contrast, PCN monotherapy lowered the hippocampal 6β-OH-TES/TES ratio, and when combined with PHT, it significantly blunted the PHT-mediated increase in TES metabolism **(Figure 3a)**. This aligns closely with PCN's previously demonstrated inhibitory action on hippocampal CYP expression.

To determine whether this restoration of TES homeostasis translates into functional improvement, additional behavioral and structural assessments were performed. In the Morris water maze, the prolonged escape latencies and reduced target quadrant exploration caused by PHT were markedly improved in animals receiving concurrent PCN **(Figure 3b)**. Likewise, PHT-induced anxiety-like behavior in the elevated plus maze—manifested as shorter open-arm duration and fewer entries—was substantially reversed by PCN co-administration **(Figure 3c)**. Open-field exploration revealed that PHT's reduction in central zone occupancy was also corrected by PCN, with no alteration in overall locomotor activity **(Figure 3d)**. Together, these results demonstrate that PCN provides robust protection against PHT-associated neurobehavioral impairments.

Golgi staining further revealed structural correlates of this protection. PHT exposure notably decreased dendritic branching and spine density in CA1 hippocampal neurons, changes that were largely prevented by PCN co-treatment (**Figure 3e,** top panels). In contrast, dendritic morphology in the DG appeared largely unaffected by either PHT alone or in combination with PCN (**Figure 3e**, bottom panels). At the molecular level, PHT suppressed transcription of key synaptic proteins (PSD95, SYN1, SYP, SYT1), and this downregulation was significantly ameliorated in the PHT + PCN group **(Figure 3f)**. These observations indicate that PCN exerts region-specific neuroprotection, primarily safeguarding CA1 neurons from PHT-induced injury.

PCN confers neuroprotection through a PXR-independent pathway

Since PCN counteracts PHT-induced hippocampal CYP elevation without requiring PXR, we next examined whether its neuroprotective benefits similarly occur independently of this receptor. Behavioral and damage markers were therefore assessed in PXR knockout mice subjected to the same treatment regimens. PHT reduced target quadrant preference in the Morris water maze among knockout animals, yet this spatial memory deficit was effectively rescued by PCN co-administration **(Figure 4a)**. In the elevated plus maze, PHT decreased both open-arm entries and dwell time in PXR-null mice, effects that were likewise reversed by PCN **(Figure 4b)**. Open-field testing showed that PHT diminished central zone exploration without altering total distance traveled, and PCN again restored normal patterns **(Figure 4c)**. Overall, these data confirm that PCN's ability to shield against PHT-related neurotoxicity operates via mechanisms unrelated to PXR signaling.

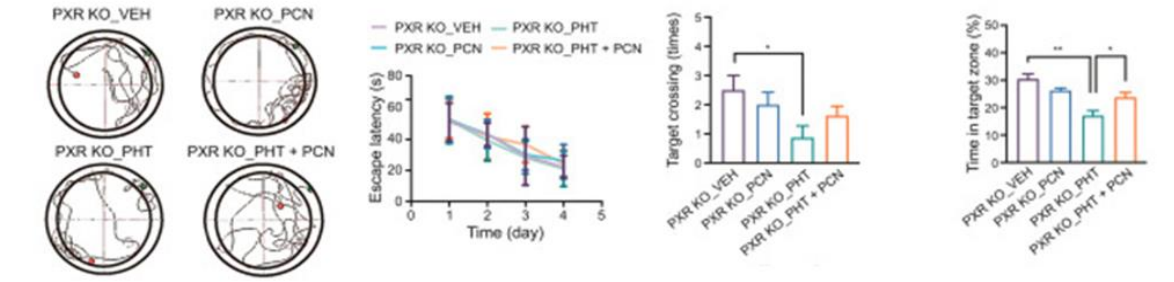

a)

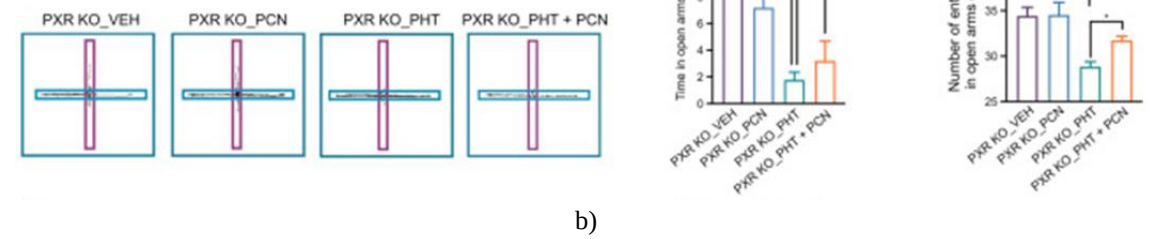

b)

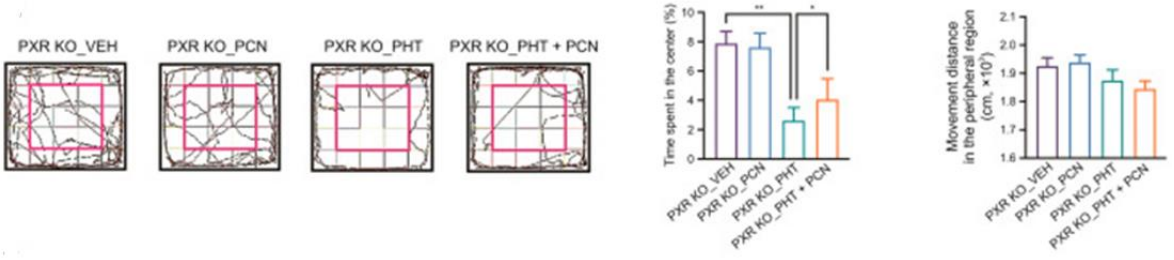

c)

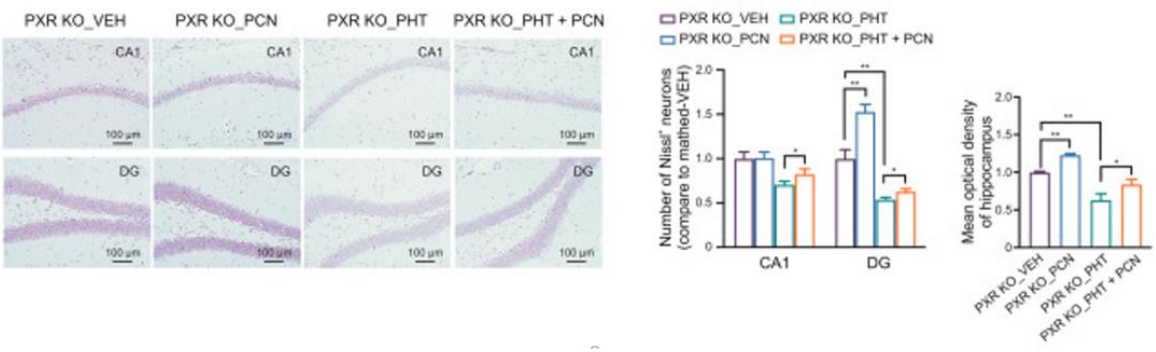

d)

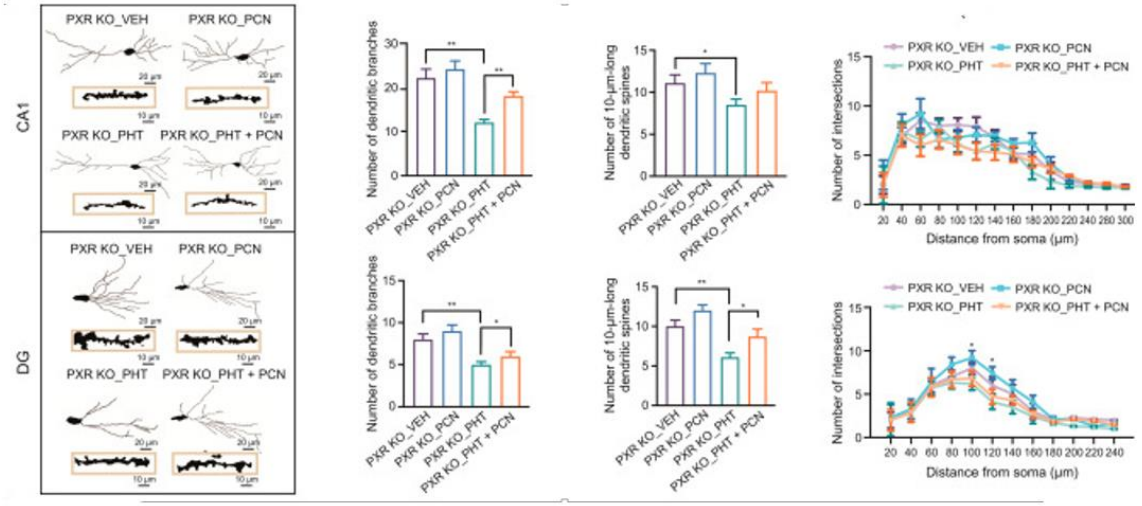

e)

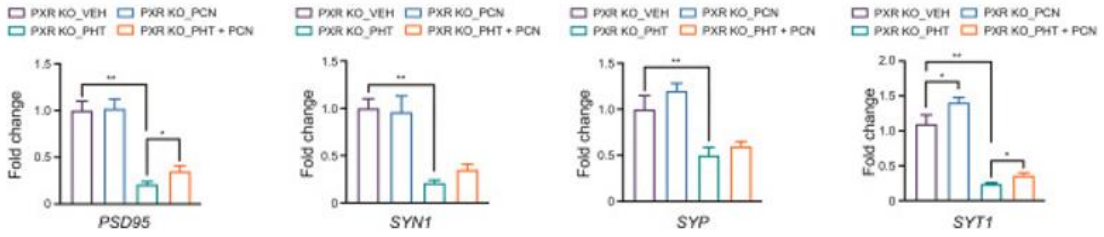

f)

Figure 4. PCN confers neuroprotection independently of PXR signaling. Male PXR-deficient (PXR KO) mice were administered vehicle (VEH), pregnenolone 16α-carbonitrile (PCN), phenytoin (PHT), or a combination of PHT and PCN for four weeks prior to evaluation (n = 6). (a) Spatial learning and memory were assessed using the Morris water maze, with escape latency, number of platform crossings, and time spent in the target quadrant quantified. (b) Anxiety-like behavior was evaluated using the elevated plus maze, including movement trajectories, duration of time spent in open arms, and number of open-arm entries. (c) Locomotor and exploratory behavior were measured in the open field test by analyzing time spent in the center zone and distance traveled along the periphery. (d) Representative Nissl-stained hippocampal sections are shown, with quantification of Nissl body–positive neurons and mean optical density. (e) Golgi-stained hippocampal sections illustrate dendritic morphology of neurons in the cornu ammonis 1 (CA1) and dentate gyrus (DG), with quantitative analysis of dendritic branch number, spine density, and branch nodes. (f) Messenger RNA (mRNA) levels of PSD95, SYN1, SYP, and SYT1 in the hippocampus were determined by real-time quantitative reverse transcription–polymerase chain reaction (RT-qPCR). Data are expressed as mean ± standard error of the mean. ∗P < 0.05, ∗∗P < 0.01.

Histological evaluation using Nissl staining demonstrated that exposure to PHT markedly reduced the number of Nissl-positive neurons in both the CA1 and DG subregions of the hippocampus in PXR KO mice. This neuronal

loss was substantially alleviated when PCN was administered concurrently with PHT **(Figure 4d)**. Quantitative analysis of staining intensity across entire hippocampal sections further revealed that PCN alone increased overall Nissl staining density, whereas PHT treatment produced a clear reduction. Importantly, mice receiving combined PHT and PCN treatment exhibited significantly greater staining intensity than those treated with PHT alone **(Figure 4d)**.

Consistent with these findings, Golgi staining showed that PHT administration significantly decreased dendritic branching and spine density in hippocampal neurons of PXR KO mice. These structural deficits were observed in both CA1 (**Figure 4e**, upper middle panels) and DG regions (**Figure 4e**, lower middle panels). Co-administration of PCN largely reversed these PHT-induced morphological alterations. Analysis of dendritic intersections revealed no significant differences among treatment groups in the CA1 region **(Figure 4e**, upper right panel). In contrast, in the DG region, the number of dendritic intersections at distances of 100 and 120 μm from the soma was significantly reduced in the PHT-treated group relative to controls **(Figure 4e**, lower right panel).

At the molecular level, PHT treatment suppressed hippocampal expression of multiple synaptic markers, including PSD95, SYN1, SYP, and SYT1, in PXR KO mice **(Figure 4f)**. Co-treatment with PCN significantly mitigated the downregulation of PSD95 and SYT1, whereas the inhibitory effects of PHT on SYN1 and SYP expression were not significantly reversed. Notably, the overall pattern of behavioral, structural, and molecular protection conferred by PCN in PXR KO mice closely resembled that observed in wild-type animals, indicating that the neuroprotective actions of PCN do not require functional PXR signaling.

Bioinformatic evidence links PHT-induced hippocampal injury to impaired GC/GR signaling

To investigate the molecular basis of PCN-mediated protection against PHT-induced neurotoxicity, we conducted a bioinformatic analysis of the publicly available GEO microarray dataset GSE2880, which compares hippocampal gene expression profiles from vehicle- and PHT-treated rats. Heatmap visualization of the top 200 differentially expressed genes (DEGs) demonstrated a clear transcriptional distinction between the two experimental groups **(Figure 5a)**.

Genes meeting the criteria of $|\log FC| > 0.5$ were selected for downstream functional enrichment analyses. Wiki pathway enrichment analysis using the ClusterProfiler package identified seven significantly altered signaling pathways, including “Glucocorticoid metabolism” and three pathways associated with G-protein–coupled receptor (GPCR) signaling **(Figure 5b)**. Emerging evidence indicates that glucocorticoids may interact with GPCRs to form functional signaling complexes with important physiological roles [32]. These findings suggest that PHT treatment disrupts glucocorticoid-related signaling networks within the hippocampus.

Consistent with this observation, Kyoto Encyclopedia of Genes and Genomes (KEGG) pathway analysis revealed significant enrichment of the “Steroid hormone biosynthesis” pathway **(Figure 5c)**. Gene set enrichment analysis further showed that this pathway was negatively enriched in the PHT-treated group, indicating a global reduction in steroid hormone biosynthetic activity **(Figure 5d)**. To corroborate these results, Gene Ontology (GO) enrichment analysis was performed, which revealed significant alterations in multiple hormone-related biological processes. Notably, terms such as “Steroid metabolic process, ” “Hormone metabolic process, ” “Steroid catabolic process, ” and “Glucocorticoid metabolic process” exhibited an upward trend **(Figure 5e)**. These findings align with previous reports demonstrating that PHT accelerates glucocorticoid metabolism, leading to reduced glucocorticoid bioavailability [33-35].

To further examine glucocorticoid receptor (GR)–associated transcriptional changes, we analyzed the expression of GR-responsive genes within the microarray dataset. Genes typically activated by GR signaling, including *Kat2b*, *Cav1*, *Per1*, *Trim63*, *Hdac1*, and *Ncoa1*, were significantly downregulated in the PHT-treated group **(Figure 5f)**. Conversely, genes commonly suppressed by GR, such as *Jun*, *AP1*, *AR*, *Atp1b1*, and *Nr4a2*, were upregulated following PHT exposure **(Figure 5g)**. In addition, expression of the GR gene itself (*Nr3c1*) was reduced in the PHT group **(Figure 5h)**.

Collectively, these transcriptomic alterations indicate that PHT-induced hippocampal neurotoxicity is closely associated with suppression of GC/GR signaling pathways. Although the analyzed dataset was derived from rats, the high degree of evolutionary conservation of GR and its downstream signaling components supports the relevance of these findings and justified a focused investigation of GR-mediated mechanisms in subsequent experimental analyses.

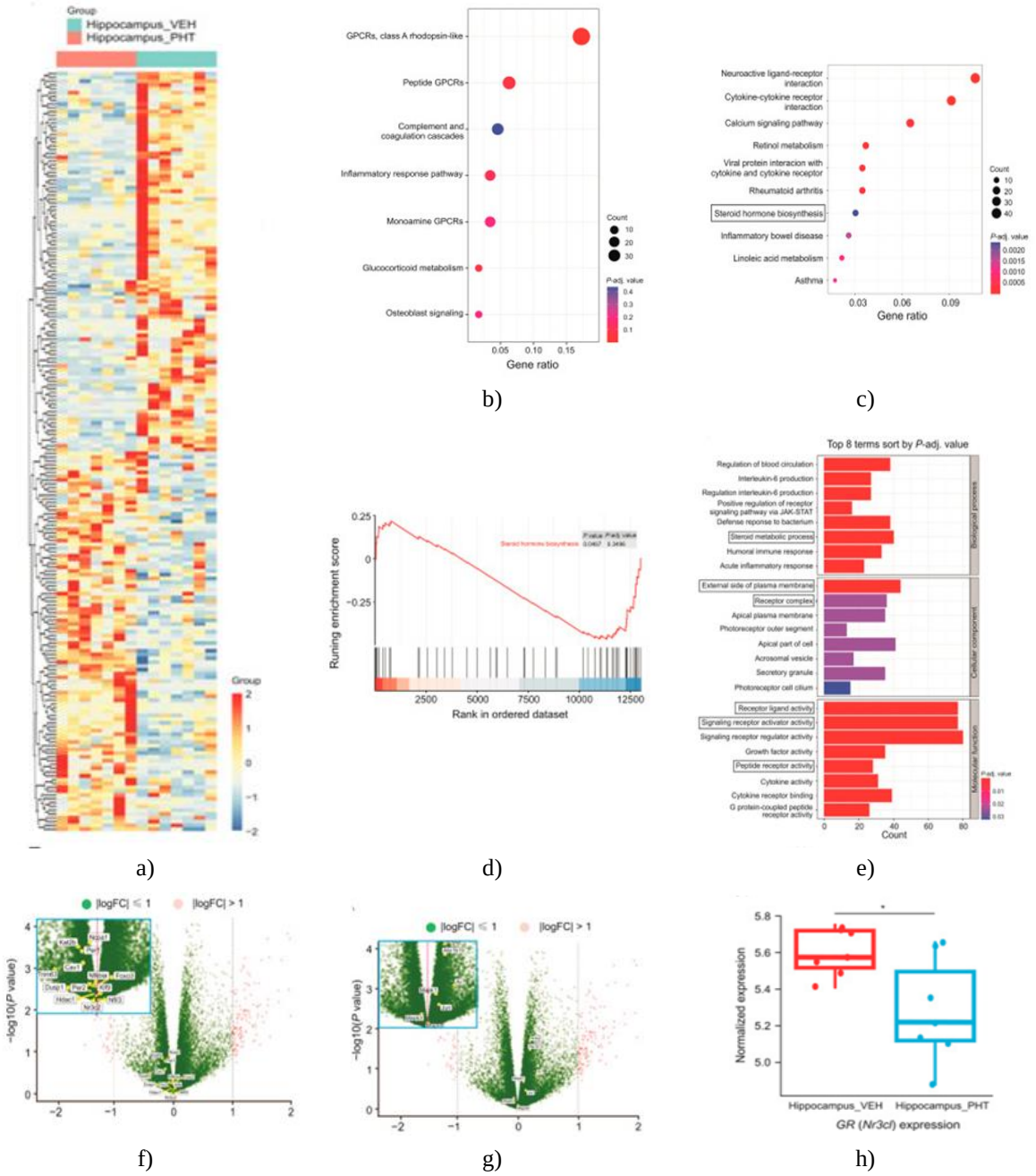

a) b) c) d) e) f) g) h)

Figure 5. Computational analysis indicates that phenytoin (PHT)-associated neurotoxicity involves dampened glucocorticoid/glucocorticoid receptor (GR) activity in the hippocampus. (a) Heatmap illustrating the 200 most variably expressed genes after PHT administration. (b) WikiPathways enrichment results for differentially expressed genes (DEGs), generated via the ClusterProfiler R package. (c, d) The 10 leading Kyoto Encyclopedia of Genes and Genomes (KEGG) pathways identified (c), alongside gene set enrichment for the 'Steroid hormone biosynthesis' category (d). (e) Gene Ontology (GO) term enrichment for DEGs; Z-scores reveal a predominant upregulation among steroid metabolism-related processes. (f, g) Volcano plots of DEGs, with genes known to be positively regulated by GR highlighted (f) or negatively regulated by GR highlighted (g). (h) Quantification of GR (Nr3c1) mRNA in hippocampal samples from vehicle (VEH)- and PHT-exposed animals. blue dots: genes with $|\log FC| \leq 1$. $*P < 0.05$. GPCRs: G-protein-coupled receptors; Red dots: genes with $|\log FC| > 1$; JAK-STAT: Janus kinase-signal transducer and activator of transcription; FC: fold change.

PCN controls hippocampal cytochrome P450 levels and protects against PHT-related neurotoxicity through stimulation of glucocorticoid/GR signaling

To determine if PCN exerts its beneficial effects by engaging the glucocorticoid/GR axis in the hippocampus, parallel studies were performed in wild-type (WT) and PXR knockout (PXR KO) mice treated with either PCN or vehicle. Hepatic transcription of classic GR-responsive genes, including ANGPTL4 and MT2, rose following PCN exposure in both strains (**Figure 6a**, left panel). Similarly, hippocampal transcripts of other GR targets—DDIT4, FKBP5, and GILZ—were elevated by PCN regardless of genotype (**Figure 6a**, right panel). Immunohistochemistry demonstrated liver-specific GR protein upregulation by PCN in WT animals only, with no change in knockouts (**Figure 6b**). In contrast, hippocampal GR protein increased after PCN administration in both CA1 and dentate gyrus subregions across WT and PXR KO mice (**Figure 6c**).

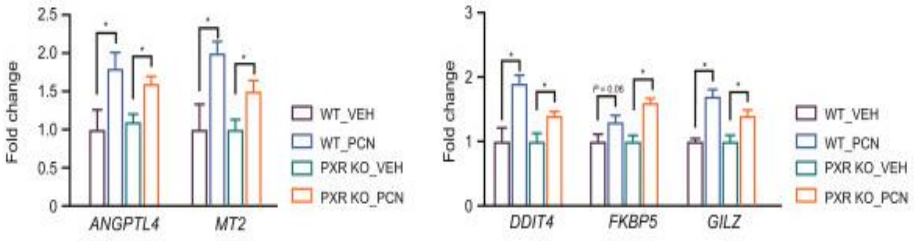

a)

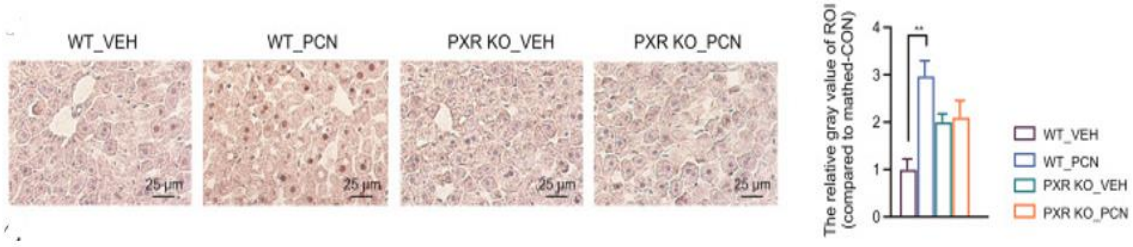

b)

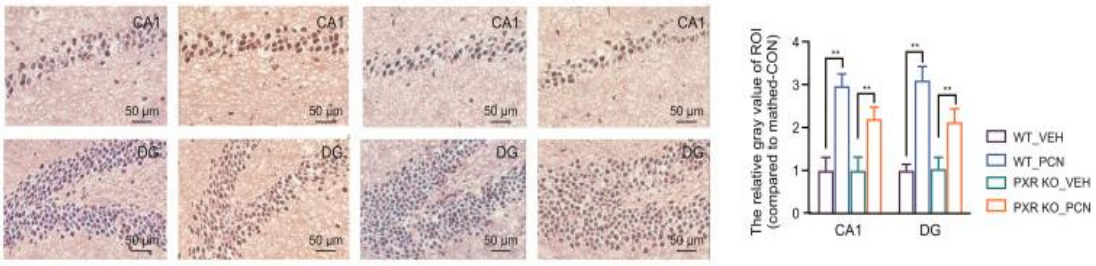

c)

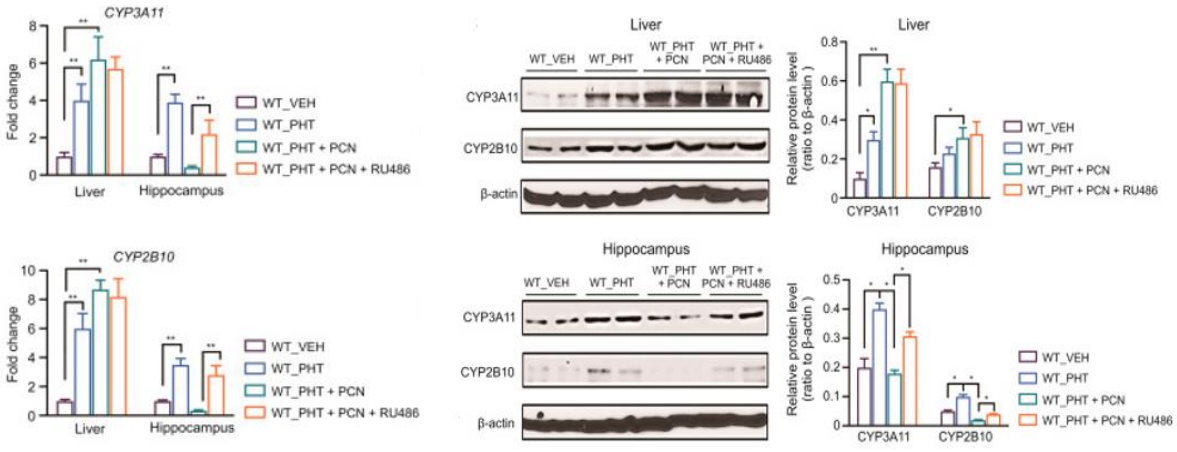

d) e)

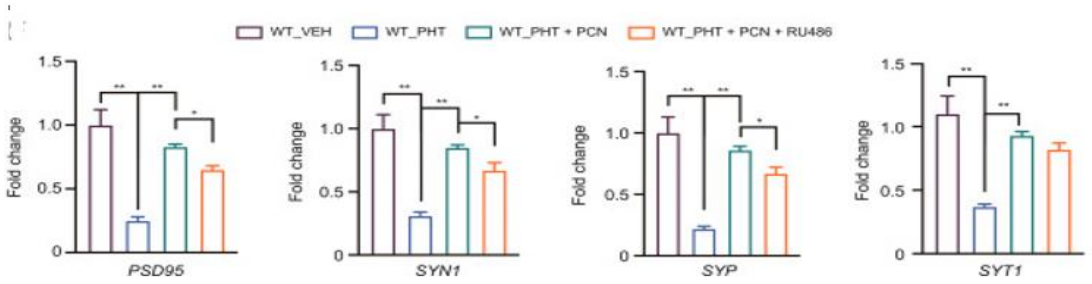

f)

Figure 6. Exposure to pregnenolone 16α-carbonitrile (PCN) triggers glucocorticoid receptor (GR) signaling without relying on pregnane X receptor (PXR), while GR engagement proves critical for PCN-driven inhibition of hippocampal cytochrome P450 enzymes and safeguarding against phenytoin (PHT)-elicited brain toxicity. (a–c) Adult male wild-type (WT) or PXR knockout (PXR KO) animals were dosed with vehicle (VEH) or PCN every day over four weeks ahead of sample harvesting (n = 6). Transcript abundance of GR-responsive genes was evaluated through RT-qPCR in hepatic tissue (a, left) and hippocampal tissue (a, right). Immunohistochemical (IHC) visualization examined GR protein distribution in liver (b) and hippocampus (c), followed by densitometric assessment via ImageJ IHC-Toolbox tools. (d–f) Wild-type male animals underwent regimens of vehicle (VEH), PHT monotherapy, PHT + PCN, or PHT + PCN + mifepristone (RU486) across four weeks (n = 6). Transcript (d) and protein (e) abundance for CYP3A11 and CYP2B10 across liver and hippocampus was quantified using RT-qPCR and Western blotting. Additionally, hippocampal transcripts for synaptic proteins PSD95, SYN1, SYP, and SYT1 were assayed via RT-qPCR (f). Values expressed as mean ± SEM. ∗P < 0.05; ∗∗P < 0.01. CON: control.

To elucidate if PCN shields wild-type animals from PHT brain toxicity via glucocorticoid/GR pathways, the antagonist mifepristone (RU486) was added alongside. Hepatic induction of CYP3A11 and CYP2B10 transcripts from PHT + PCN remained largely unaffected by RU486 **(Figure 6d)**. However, in hippocampal regions, RU486 fully negated PCN's restraint on PHT-boosted CYP3A11 and CYP2B10 transcription **(Figure 6d)**, underscoring GR's pivotal role in PCN's region-selective control over cytochrome P450. Protein assessments by Western blotting echoed this: minimal hepatic influence from RU486 (**Figure 6e**, top panels), yet complete blockade of PCN's hippocampal CYP-lowering action (**Figure 6e**, bottom panels). Synaptic transcript profiling revealed PCN offset PHT's repression of PSD95, SYN1, and SYP in hippocampus, but RU486 co-delivery substantially eroded this benefit for those markers **(Figure 6f)**.

To test if targeted GR stimulation alone can mimic PCN's defense against PHT-triggered conduct issues and hippocampal harm—while checking PXR independence—WT and PXR KO groups received the GR agonist dexamethasone (DEX) at 4 mg/kg/day, chosen for GR-specificity over PXR crossover [36]. DEX boosted GR target transcripts in liver and hippocampus across both strains **(Figure 7a**, left panels), validating PXR-free GR engagement. Hippocampally, DEX replicated PCN by markedly curbing CYP3A11 and CYP2B10 levels in either genotype (**Figure 7a**, right panels). DEX also enhanced hippocampal synaptic gene transcription (PSD95, SYN1, SYP, SYT1) similarly in WT and knockout animals **(Figure 7b)**, aligning tightly with PCN outcomes. Confirming GR mediation in knockouts, DEX + RU486 pairing was examined: DEX overturned PHT-elevated hippocampal CYP3A11/CYP2B10, yet RU486 nullified this. Likewise, DEX's partial rescue of PHT-dampened synaptic transcripts vanished with RU486.

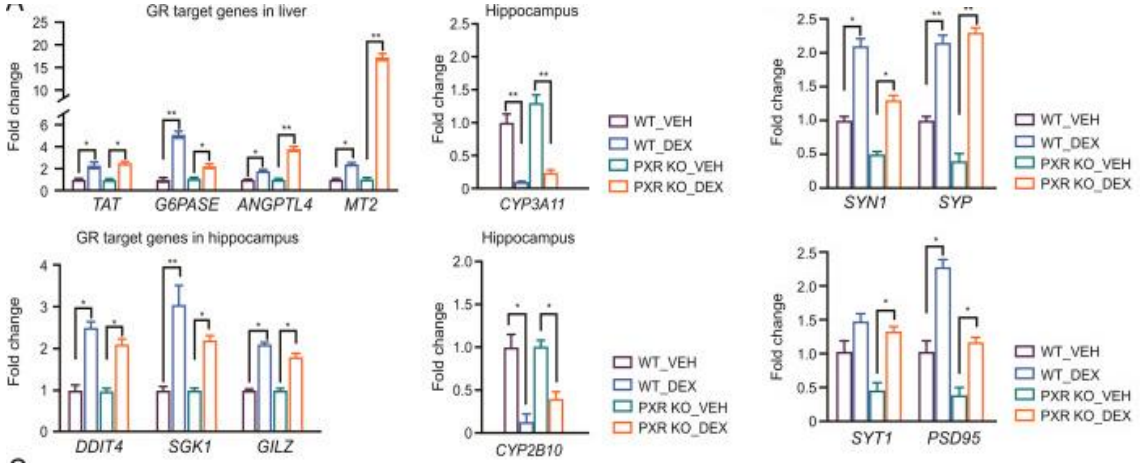
GR target genes in liver
Fold change
TAT
G6PASE
ANGPTL4
MT2
Hippocampus
CYP3A11
SYN1
SYP
GR target genes in hippocampus
DDIT4
SGK1
GILZ
CYP2B10
SYT1
PSD95
WT_VEH
WT_DEX
PXR KO_VEH
PXR KO_DEX

a) b)

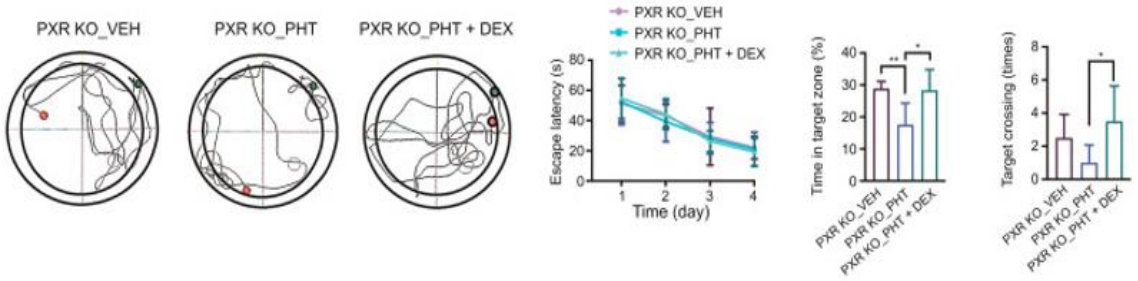
PXR KO_VEH
PXR KO_PHT
PXR KO_PHT + DEX
Escape latency (s)
Time (day)
Time in target zone (%)
Target crossing (times)

c)

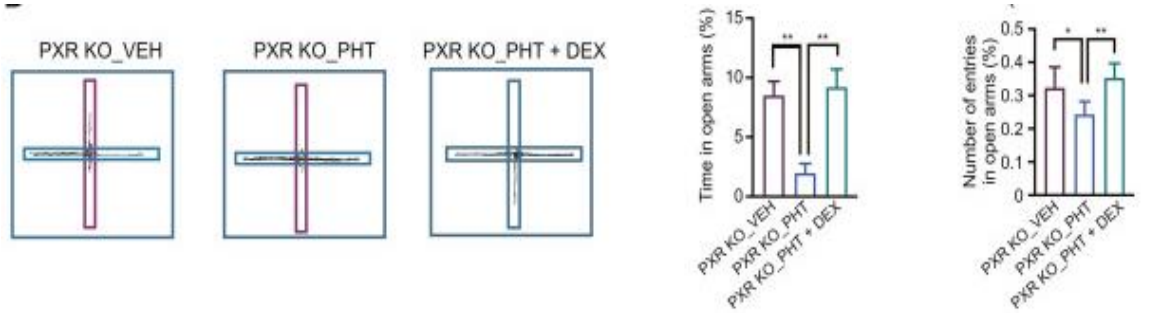
PXR KO_VEH
PXR KO_PHT
PXR KO_PHT + DEX
Time in open arms (%)
Number of entries in open arms (%)

d)

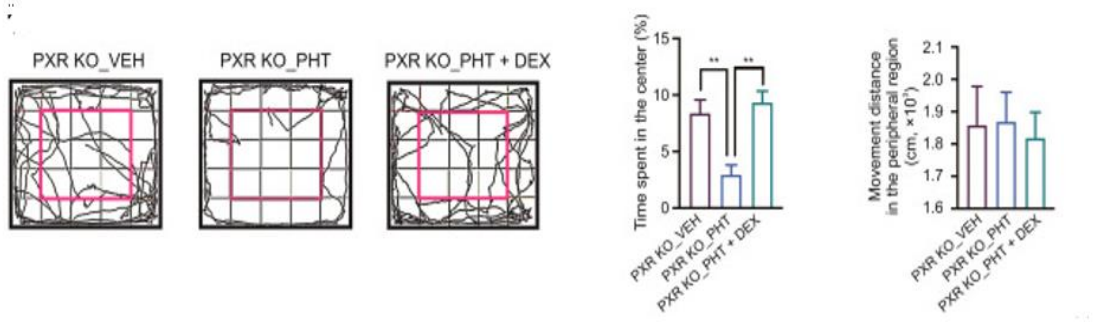
PXR KO_VEH
PXR KO_PHT
PXR KO_PHT + DEX
Time spent in the center (%)
Movement distance in the peripheral region (cm, ×10³)

e)

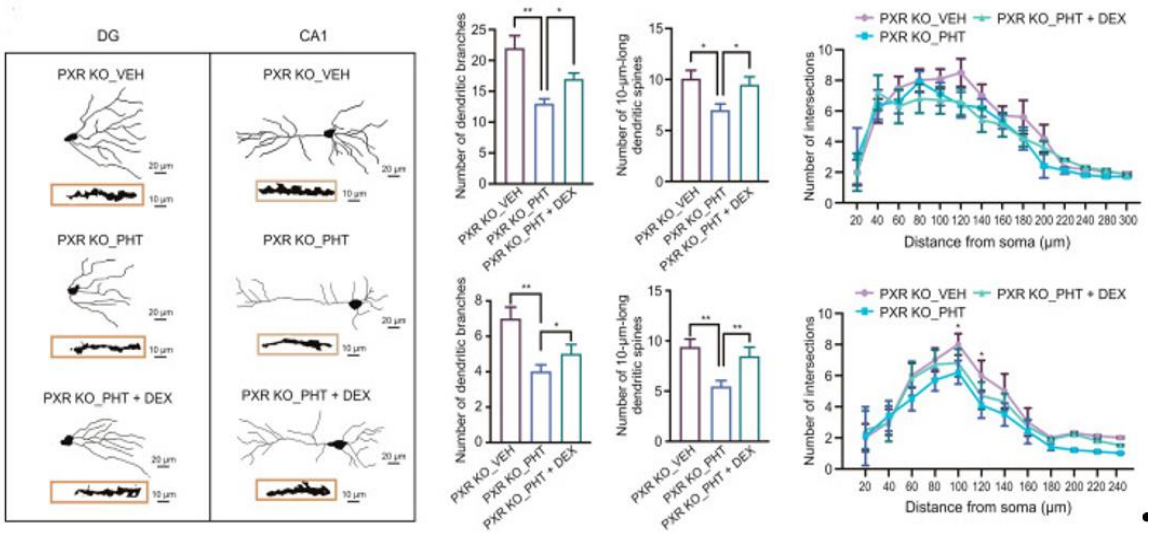

f)

Figure 7. Direct pharmacological stimulation of the glucocorticoid receptor (GR) effectively counters phenytoin (PHT)-induced neurotoxicity without involvement of pregnane X receptor (PXR). (a, b) Adult male wild-type (WT) or PXR knockout (PXR KO) mice received vehicle (VEH) or dexamethasone (DEX) daily for four weeks prior to sample collection (n = 8). mRNA levels of GR-responsive genes were quantified by RT-qPCR in liver and hippocampal tissues (A, left panels). Hippocampal transcripts for CYP3A11 and CYP2B10 (a, right panels) as well as synaptic markers PSD95, SYN1, SYP, and SYT1 (b) were also measured via RT-qPCR. (C–F) Male PXR KO mice underwent treatment with vehicle, PHT alone, or PHT + DEX for four weeks (n = 6). Morris water maze performance included escape latency tracking, platform crossings, and target quadrant dwell time (c). Elevated plus maze metrics encompassed movement traces, open-arm duration, and entries (d). Open-field assessment recorded central zone occupancy and peripheral distance traveled (e). Golgi-impregnated hippocampal sections provided neurite tracings from CA1 and dentate gyrus (DG) neurons, with quantification of dendritic branches, spine density, and intersections (f). Results are displayed as mean ± SEM. ∗P < 0.05; ∗∗P < 0.01.

The impact of DEX on PHT-triggered behavioral deficits and hippocampal damage was examined in PXR knockout animals. In the Morris water maze, PHT shortened target quadrant exploration time in knockouts, an impairment that DEX co-administration fully restored **(Figure 7c)**. Elevated plus maze testing revealed PHT-reduced open-arm dwell time and entries, both of which were normalized by concurrent DEX **(Figure 7d)**. Open-field exploration showed PHT lowered central area occupancy while leaving overall locomotion unchanged; DEX again corrected this pattern **(Figure 7e)**. Golgi analysis of hippocampal morphology in PXR KO mice demonstrated that PHT diminished dendritic branching and spine density in the CA1 subfield (without altering intersection counts), changes largely prevented by DEX (**Figure 7f**, upper panels). In the dentate gyrus, PHT decreased spine density along with branch number and intersections, effects similarly mitigated by DEX co-delivery (**Figure 7f**, lower panels). Collectively, these findings indicate that a GR-selective dose of DEX provides robust protection against PHT-associated neurotoxicity through mechanisms unrelated to PXR.

This study yielded several findings that were not anticipated at the outset. First, we observed a striking divergence in the effects of pregnenolone 16α-carbonitrile (PCN) on cytochrome P450 (CYP) expression between peripheral and central tissues. PCN is widely recognized as a potent activator of pregnane X receptor (PXR) and has been extensively documented to induce hepatic CYP expression through PXR-dependent mechanisms [16], a phenomenon that was again confirmed here. In contrast, and unexpectedly, the same PCN treatment resulted in marked down-regulation of CYP3A11 and CYP2B10 expression within the hippocampus. To our knowledge, this represents the first evidence that PCN can exert tissue-specific and even opposing regulatory effects on CYP expression.

A second unanticipated observation concerned the mechanism underlying PCN-mediated suppression of hippocampal CYPs. Although PCN classically functions as a PXR agonist, our data clearly demonstrate that its inhibitory effect on hippocampal CYP expression does not require PXR activity. This conclusion is supported by

the finding that PCN retained its suppressive capacity in PXR knockout (PXR KO) mice. Instead, transcriptomic analyses combined with pharmacological intervention using the glucocorticoid receptor (GR) antagonist RU486 revealed that GR activation is central to this process. Specifically, blockade of GR signaling abolished the inhibitory effect of PCN on hippocampal CYP expression, while administration of the GR agonist dexamethasone (DEX) alone was sufficient to repress these CYPs. Together, these findings suggest that activation of GR signaling mediates the hippocampal actions of PCN and raise the possibility that glucocorticoid co-therapy could be explored as an approach to mitigate the neuronal adverse effects associated with phenytoin (PHT). Notably, glucocorticoids have already been used as adjunctive therapies in epilepsy syndromes and in cases of drug-resistant epilepsy [37, 38].

Cytochrome P450 enzymes, including members of the CYP3A, CYP2B, and CYP2C subfamilies, are traditionally studied in the context of hepatic and intestinal metabolism, where their roles in xenobiotic clearance are well established [1, 39]. Our findings provide compelling evidence that these CYP isoforms are also expressed and transcriptionally regulated within the central nervous system. Importantly, hippocampal CYPs may influence local metabolism of endogenous substrates, such as androgens, and potentially contribute to the cerebral disposition of drugs and environmental chemicals.

From a clinical perspective, these observations are highly relevant. PHT therapy is well known to be associated with neuropsychiatric side effects, including anxiety, learning deficits, and cognitive impairment [40-43], all of which were reproduced in our animal model. Mechanistically, our data strongly support the notion that PHT-induced behavioral abnormalities and hippocampal neurotoxicity arise from the induction of hippocampal CYPs, leading to accelerated metabolic inactivation of testosterone (TES). TES is a neuroactive steroid that plays a critical role in regulating mood, cognition, and behavior [44]. The hypothesis that reduced TES contributes to the adverse neurological effects of PHT is consistent with prior evidence linking diminished central TES levels to PHT-associated neurotoxicity [29]. Clinically, male patients with temporal lobe epilepsy exhibit significantly reduced concentrations of bioavailable TES—including both free and albumin-bound fractions—accompanied by symptoms such as decreased libido, erectile dysfunction, depression, and cognitive decline [45, 46]. Notably, these manifestations are more pronounced in individuals treated with enzyme-inducing antiepileptic drugs, such as PHT, compared with those receiving non-inducing therapies [6, 28]. Furthermore, alterations in TES levels appear to be more prominent in the hippocampus than in circulation [47], underscoring the importance of hippocampal CYPs in local steroid metabolism and implicating them in the neurotoxic side effects of antiepileptic medications.

Several limitations of the present study should be acknowledged. First, as illustrated in **Figures 3 and 4**, PCN effectively normalized synaptic gene expression and improved anxiety-, depression-, learning-, and memory-related behaviors in PHT-treated wild-type mice. However, Golgi staining revealed that structural recovery was primarily confined to the CA1 region of the hippocampus, with limited effects observed in the dentate gyrus (DG). This discrepancy may reflect the relatively modest DG pathology induced by PHT in our experimental model. In contrast, in PXR KO mice, PCN ameliorated neuronal damage in both CA1 and DG regions, possibly because PHT caused more extensive hippocampal injury in the absence of PXR, thereby allowing greater scope for PCN-mediated recovery.

Second, while our data indicate that PCN activates GR signaling in the hippocampus, its effects on hepatic GR remain unclear. Earlier studies suggested that PCN may antagonize GR activity in the liver [48]. Whether such tissue-specific modulation of GR contributes to the opposing effects of PCN on CYP expression in liver versus hippocampus will require further investigation, ideally using tissue-specific GR knockout models.

Third, although PCN effectively reduced PHT-induced neurotoxicity in the current study, its neuroprotective efficacy has not yet been evaluated in a bona fide epilepsy model, which will be essential for assessing translational relevance.

Fourth, the possible involvement of constitutive androstane receptor (CAR) cannot be excluded. PHT has been shown to induce CYP expression through CAR activation [13], and future studies employing CAR knockout mice will be necessary to definitively delineate its contribution to PHT-induced neurotoxicity and the mitigating effects of PCN.

Finally, species-specific differences in nuclear receptor regulation and responsiveness represent an additional limitation. Caution is therefore warranted when extrapolating these findings to humans, and further studies are needed to assess clinical applicability.

Conclusion

In conclusion, this study demonstrates that PCN, a prototypical PXR agonist, exerts a previously unrecognized tissue-specific inhibitory effect on CYP expression within the hippocampus. By suppressing hippocampal CYPs and preserving testosterone bioactivity through activation of glucocorticoid/GR signaling, PCN confers protection against PHT-induced hippocampal neuronal injury. Although PCN itself is not used clinically, these findings highlight glucocorticoid signaling as a potential therapeutic target for alleviating the neurological side effects associated with phenytoin treatment.

Acknowledgments: None

Conflict of Interest: None

Financial Support: None

Ethics Statement: None

References

1. Anzenbacher P, Anzenbacherová E. Cytochromes P450 and metabolism of xenobiotics. Cell Mol Life Sci. 2001;58:737–47.
2. Kuban W, Daniel WA. Cytochrome P450 expression and regulation in the brain. Drug Metab Rev. 2021;53:1–29.
3. Schilter B, Omiecinski CJ. Regional distribution and expression modulation of cytochrome P-450 and epoxide hydrolase mRNAs in the rat brain. Mol Pharmacol. 1993;44:990–6.
4. Miksys SL, Tyndale RF. Drug-metabolizing cytochrome P450s in the brain. J Psychiatry Neurosci. 2002;27:406–15.
5. Herzog AG, Levesque LA, Drislane FW, Boushell DW, Rudd AD. Phenytoin-induced elevation of serum estradiol and reproductive dysfunction in men with epilepsy. Epilepsia. 1991;32:550–3.
6. Isojärvi JIT, Taubøll E, Herzog AG. Effect of antiepileptic drugs on reproductive endocrine function in individuals with epilepsy. CNS Drugs. 2005;19:207–23.
7. Quartier A, Chatrousse L, Redin C, Keime C, Hitte C, Renard E, et al. Genes and pathways regulated by androgens in human neural cells, potential candidates for the male excess in autism spectrum disorder. Biol Psychiatry. 2018;84:239–52.
8. Ransome MI, Boon WC. Testosterone-induced adult neurosphere growth is mediated by sexually-dimorphic aromatase expression. Front Cell Neurosci. 2015;9.
9. Spritzer MD, Galea LAM. Testosterone and dihydrotestosterone, but not estradiol, enhance survival of new hippocampal neurons in adult male rats. Dev Neurobiol. 2007;67:1321–33.
10. Benice TS, Raber J. Castration and training in a spatial task alter the number of immature neurons in the hippocampus of male mice. Brain Res. 2010;1329:21–9.
11. Corona G, Guaraldi F, Rastrelli G, Vignozzi L, Saracino V, Sforza A, et al. Testosterone deficiency and risk of cognitive disorders in aging males. World J Mens Health. 2021;39:9–18.
12. Kurth F, Luders E, Sicotte NL, Gaser C, Giesser BS, Swerdloff RS, et al. Neuroprotective effects of testosterone treatment in men with multiple sclerosis. Neuroimage Clin. 2014;4:454–60.
13. Wang H, Faucette S, Moore R, Sueyoshi T, Negishi M, LeCluyse E, et al. Human constitutive androstane receptor mediates induction of CYP2B6 gene expression by phenytoin. J Biol Chem. 2004;279:29295–301.
14. Jackson JP, Ferguson SS, Moore R, Negishi M, Goldstein JA. The constitutive active/androstane receptor regulates phenytoin induction of Cyp2c29. Mol Pharmacol. 2004;65:1397–404.
15. Torres-Vergara P, Ho YS, Espinoza F, García-Rojo G, Aránguiz A, Escudero C, et al. The constitutive androstane receptor and pregnane X receptor in the brain. Br J Pharmacol. 2020;177:2666–82.
16. Xie W, Barwick JL, Downes M, Blumberg B, Simon CM, Nelson MC, et al. Humanized xenobiotic response in mice expressing nuclear receptor SXR. Nature. 2000;406:435–9.

17. Applegate CD, Samoriski GM, Özduman K, Spencer DD. Effects of valproate, phenytoin, and MK-801 in a novel model of epileptogenesis. Epilepsia. 1997;38:631–6.
18. Sudha S, Lakshmana MK, Pradhan N. Chronic phenytoin induced impairment of learning and memory with associated changes in brain acetylcholinesterase activity and monoamine levels. Pharmacol Biochem Behav. 1995;52:119–24.
19. Mohan A, Krishna K. Memory impairment allied to temporal lobe epilepsy and its deterioration by phenytoin: A highlight on ameliorative effects of levetiracetam in mouse model. Int J Epilepsy. 2018;5:19–27.
20. Zoufal V, Mairinger S, Brackhan M, Krohn M, Neddens J, Mueller M, et al. Imaging P-glycoprotein induction at the blood-brain barrier of a β-amyloidosis mouse model with 11C-metoclopramide PET. J Nucl Med. 2020;61:1050–7.
21. Bauer B, Hartz AM, Fricker G, Miller DS. Pregnane X receptor up-regulation of P-glycoprotein expression and transport function at the blood-brain barrier. Mol Pharmacol. 2004;66:413–9.
22. Yılmaz T, Akça M, Turan Y, Akyüz C, Akyüz M, Kaya M, et al. Efficacy of dexamethasone on penicillin-induced epileptiform activity in rats: An electrophysiological study. Brain Res. 2014;1554:67–72.
23. Zhang Y, Hu W, Zhang B, Zhao X, Li Y, Chen G, et al. Ginsenoside Rg1 protects against neuronal degeneration induced by chronic dexamethasone treatment by inhibiting NLRP-1 inflammasomes in mice. Int J Mol Med. 2017;40:1134–42.
24. Peeters BW, Tonnaer JA, Groen MB, van Dijk CW, van der Zee EA, et al. Glucocorticoid receptor antagonists: New tools to investigate disorders characterized by cortisol hypersecretion. Stress. 2004;7:233–41.
25. Shu J, Qiu G, Mohammad I, Zhang L, Wang Y. Semi-automatic image analysis tool for biomarker detection in immunohistochemistry analysis. In: Proceedings of the 2013 Seventh International Conference on Image and Graphics (ICIG). IEEE; 2013. p. 937–942.
26. Konkle ATM, McCarthy MM. Developmental time course of estradiol, testosterone, and dihydrotestosterone levels in discrete regions of male and female rat brain. Endocrinology. 2011;152:223–35.
27. DuBois BN, Amirrad F, Mehvar R. A comparison of calcium aggregation and ultracentrifugation methods for the preparation of rat brain microsomes for drug metabolism studies. Pharmacology. 2021;106:687–92.
28. Jeavons PM. Letter: Behavioural effects of anti-epileptic drugs. Dev Med Child Neurol. 1976;18:394.
29. Meyer RP, Hagemeyer CE, Knoth R, Ehrlich H, Heinemann A, Hohmann A, et al. Anti-epileptic drug phenytoin enhances androgen metabolism and androgen receptor expression in murine hippocampus. J Neurochem. 2006;96:460–72.
30. Ghosh C, Hossain M, Spriggs A, Williams A, Moghaddam B, Lothman E, et al. Sertraline-induced potentiation of the CYP3A4-dependent neurotoxicity of carbamazepine: An in vitro study. Epilepsia. 2015;56:439–49.
31. Niwa T, Murayama N, Imagawa Y, Yamazaki H. Regioselective hydroxylation of steroid hormones by human cytochromes P450. Drug Metab Rev. 2015;47:89–110.
32. Ping YQ, Mao C, Xiao P, Zhang G, Zhang Y, Wang Y, et al. Structures of the glucocorticoid-bound adhesion receptor GPR97-Go complex. Nature. 2021;589:620–6.
33. Kara C, Ucaktürk A, Aydın OF, Aydin S, Darcan S. Adverse effect of phenytoin on glucocorticoid replacement in a child with adrenal insufficiency. J Pediatr Endocrinol Metab. 2010;23:963–6.
34. Chalk JB, Ridgeway K, Brophy T, McGowan S, Wesselingh S. Phenytoin impairs the bioavailability of dexamethasone in neurological and neurosurgical patients. J Neurol Neurosurg Psychiatry. 1984;47:1087–90.
35. Jubiz W, Meikle AW. Alterations of glucocorticoid actions by other drugs and disease states. Drugs. 1979;18:113–21.
36. Hunter SR, Vonk A, Mullen Grey AK, Mahnke A, Geiger SD, Bae SH, et al. Role of glucocorticoid receptor and pregnane X receptor in dexamethasone induction of rat hepatic aryl hydrocarbon receptor nuclear translocator and NADPH-cytochrome P450 oxidoreductase. Drug Metab Dispos. 2017;45:118–29.
37. Haberlandt E, Weger C, Sigl SB, Rauchenzauner M, Scholl-Bürgi S, Rostásy K, et al. Adrenocorticotropic hormone versus pulsatile dexamethasone in the treatment of infantile epilepsy syndromes. Pediatr Neurol. 2010;42:21–7.
38. Shorvon S, Ferlisi M. The treatment of super-refractory status epilepticus: A critical review of available therapies and a clinical treatment protocol. Brain. 2011;134:2802–18.

39. Thelen K, Dressman JB. Cytochrome P450-mediated metabolism in the human gut wall. J Pharm Pharmacol. 2009;61:541–58.
40. Kanner AM, Bicchi MM. Antiseizure medications for adults with epilepsy: A review. JAMA. 2022;327:1269–81.
41. Patocka J, Wu Q, Nepovimova E, Kuca K. Phenytoin–An anti-seizure drug: overview of its chemistry, pharmacology and toxicology. Food Chem Toxicol. 2020;142:111–8.
42. Cardoso-Vera JD, Gómez-Oliván LM, Islas-Flores H, García-Medina S, Elizalde-Velázquez GA, Orozco-Hernández JM, et al. Multi-biomarker approach to evaluate the neurotoxic effects of environmentally relevant concentrations of phenytoin on adult zebrafish Danio rerio. Sci Total Environ. 2022;834:155220.
43. Nagib MM, Tadros MG, Rahmo RM, Khalifa AE, El-Sayed NM. Ameliorative effects of α-tocopherol and/or coenzyme Q10 on phenytoin-induced cognitive impairment in rats: Role of VEGF and BDNF-TrkB-CREB pathway. Neurotox Res. 2019;35:451–62.
44. McEwen BS. How do sex and stress hormones affect nerve cells? Ann N Y Acad Sci. 1994;743:1–18.
45. Herzog AG, Fowler KM. Sexual hormones and epilepsy: Threat and opportunities. Curr Opin Neurol. 2005;18:167–72.
46. Frye CA. Role of androgens in epilepsy. Expert Rev Neurother. 2006;6:1061–75.
47. Killer N, Hock M, Gehlhaus M, Capetian P, Knoth R, Pantazis G, et al. Modulation of androgen and estrogen receptor expression by antiepileptic drugs and steroids in hippocampus of patients with temporal lobe epilepsy. Epilepsia. 2009;50:1875–90.
48. Schuetz EG, Schmid W, Schutz G, Brimer C, Yasuda K, Kamataki T, et al. The glucocorticoid receptor is essential for induction of cytochrome P-4502B by steroids but not for drug or steroid induction of CYP3A or P-450 reductase in mouse liver. Drug Metab Dispos. 2000;28:268–78.